JPE 17-4-2

https://doi.org/10.6113/JPE.2017.17.4.860
ISSN(Print): 1598-2092 / ISSN(Online): 2093-4718

A Direct Single-phase Quasi-resonant AC-AC Converter with Zero Voltage Switching

Mihail Hristov Antchev†

†Faculty of Electronic Engineering and Technology, Technical University-Sofia, Sofia, Bulgaria

Abstract

The present article reports an analysis and investigation of a direct AC-AC quasi-resonant converter. A bidirectional power device, whose switching frequency is lower than the frequency of the current passing through the load, is used for its realization. The zero voltage switching mode is described when zero voltage on the power device is available by measuring it with the control system. The continuous current in the resonant inductance by switching the power device at zero voltage is considered, and it is characterized by two sub-modes. A mathematical analysis of the processes has been made and comparative results from the computer simulation and experimental study have been brought. The converter can be used in a wide areas of power electronics: induction heating, wireless power transfer, AC-DC converters, etc.

Key words: Bidirectional switch, Direct AC-AC converter, Quasi-resonant, Zero voltage switching

I. INTRODUCTION

The standard method for converting AC into AC power is by using so called frequency converters. These converters consist of a rectifier and an inverter. The rectifier output voltage supplies the inverter where the output obtains alternating voltage for the load. This method consists of the double conversion of energy associated with reduced efficiency. To increase the energy efficiency, other types of converters exist. Some of them are well-known matrix converters which convert AC into AC power [1]-[5].

Depending on their power circuit, matrix converters are direct or indirect, with the same or different numbers of input and output phases. There are also resonant matrix converters that contain several bidirectional power devices [6], [7]. Cycloconverters are also known for converting AC into AC power, which in the standard case containing controlled rectifiers. The use of bidirectional power devices allows for the development of new schemes for high frequency cycloconverters [8], [9].

To convert AC to AC power, resonant converters based on the so called "Class E - inverter" are also used [10]-[12]. They are based on the “soft switching” technique, which makes it possible to reduce the losses of switching power devices and to increase efficiency [13]-[15]. These converters contain a different number of bidirectional power devices. The converter described in [10] contains one power device and it is designed for induction heating applications. An analysis was done on the assumption that the converter is supplied with a constant voltage, whose value is equal to the effective value of the input voltage, which does not correspond to the actual physical action. It uses "multicycle modulation," which allows for discrete power regulation at the load. However, the variable switching frequency deteriorates the electromagnetic compatibility. The authors of [16] described a direct AC-AC resonant converter, which uses two bidirectional power devices. The converter described in [17], [18] uses four power devices. At active intervals the serial resonant circuit is switched to the source of the input voltage. The bidirectional flyback converter, which in discrete moments injects energy into the resonant circuit, is described in [19]. The converter uses three power devices and the advantage is a reduced switching frequency.

To reduce the switching losses in direct conversion is using the switching technique at zero current (ZCS), the output current fluctuations are described in [18]. In [20], the same authors described a direct converter composed of four power devices. Two of them are switching the series resonant circuit to the variable supply voltage in certain periods. During the rest of the periods the other two power devices connect this circuit in short and it results in declining fluctuations. A one-

Manuscript received Oct. 11, 2016; accepted Apr. 1, 2017
Recommended for publication by Associate Editor Sangshin Kwak.
†Corresponding Author: antchev@tu-sofia.bg
Tel: +359 2 965 3321, Technical University-Sofia

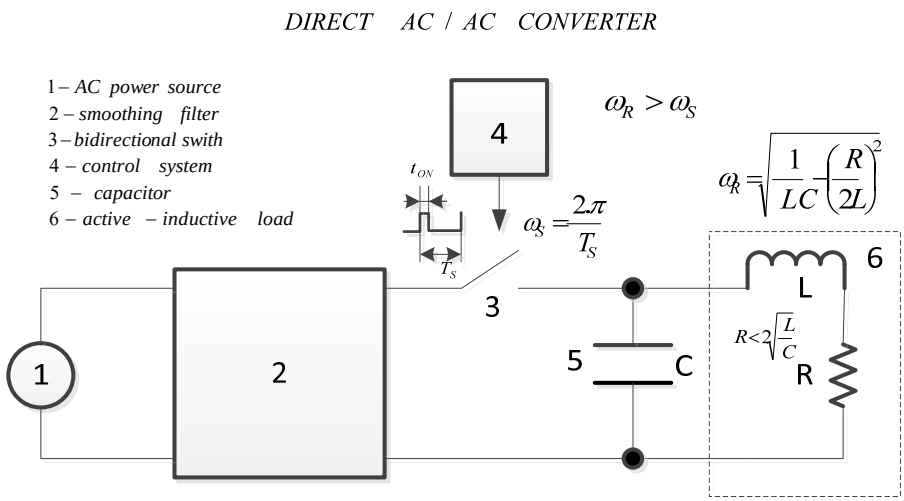

Fig. 1. Block diagram of an AC-AC quasi-resonant converter.

phase voltage direct three-phase converter is described in [21]. It also uses the ZCS technique. The three-phase to three-phase converter, described in [22] uses power devices without reverse conductivity. It is connected as a virtual converter and the increased efficiency is presented. A pulse density modulation technique to realize soft commutation is proposed in [23] for optimization of the power factor using a genetic algorithm.

Switching at zero voltage (ZVS) is also well known to reduce the losses on resonance switches. It is worth mentioning that the use of such switching in direct AC converters results in a limited voltage, because the principle of action does not involve a regime of standard ZVS. The aim of the study in this paper is to provide the possibility to turn-on the bidirectional power device at zero voltage in a direct converter. This switching method is different from the well-known principle. It consists of the following: the control electrode of the power device has a pulse for switching. However, since the processes in the power circuit conducts the inverse diode of the device, and after the decreasing of the current through it to 0, the transistor starts conducting. A converter with one bidirectional power device in the ZVS mode, as shown in Fig. 1 [24], is the subject of study in this paper.

The scheme is similar to the one described in [10]. Its main elements are: an AC power source (1), a bidirectional switch (3), a resonant circuit consisting of a capacitor (5) and an active-inductive load (6). The on/off switching of the device is done via a control system (4), which monitors the device voltage. The smoothing filter (2) prevents the infiltration of high-frequency interference to the power source.

The converter shown in Fig. 1 can operate in two modes:

1. "Discontinuous current mode" through the resonant inductance L. It acquires a large attenuation $\delta = \frac{R}{2.L}$ in the resonance circuit. During the switching on of the power device, the capacitor C is charged to the instantaneous value of the power supply's voltage u_S. During the switching off of the power device, the resonant circuit develops decreased oscillations. As a result, before the next time, the current is dropped to 0 and the capacitor is discharged. It is clear that in this mode, it is impossible to achieve switching on the power device at zero voltage. It is always like that before each subsequent subinterval of switching on. The voltage on the capacitor C is equal to 0 and the voltage to the left of the power switch (3) is equal to the instantaneous value of the voltage of the power source. This mode is not considered in this paper.
2. "Continuous current mode" through the resonant inductance L. It is obtained on a low attenuation $\delta = \frac{R}{2.L}$ in the resonance circuit. The capacitor C is charged to the instantaneous value of the power supply's voltage u_S after switching on the power device. When switching off the power device, decreased oscillations are developed in the resonant circuit. As a result, before switching on again, the current is not dropped to 0, and the voltage on the capacitor C continues changing. In this case, it is possible to achieve switching on of the power device under zero voltage. This process differs from the standard ZVS, where the gate of the device has a signal for the switching on. However, its reverse diode conducts, and the transistor only starts conducting when the current in the diode goes to zero. In the mode described in this paper, the voltage over the power device is monitored via the control system. The algorithm is as follows. The system (4) receives the signal u_{CG} for switching on from the generator. However, the signal for the power device u_{CD} is generated only after the voltage on of the device is 0V, i.e. when the voltage on the capacitor C and the voltage at the output of block (2) have equal values.

Part II of this paper contains mathematical descriptions of the processes in the scheme. The following basic dependencies are outlined: the current through the resonant inductance and the power device, and the voltage over the resonant capacitor C. In part III a computer simulation

study is presented. Part IV shows the results of the experimental research. Part V draws some conclusions, with attention on the main achievements and contributions of the paper.

II. MATHEMATICAL DESCRIPTION

The scheme with marked variables used in this mathematical description and experimental studies is shown in Fig. 2. As an anti-interference filter is shown the LC filter - L_F, C_F. However, its configuration can be different. This filter is ignored in the mathematical description, because the main purpose is to examine the ZVS mode.

As previously mentioned, the continuous current in the resonant inductance by switching the power device at zero voltage is considered. This is characterized by two sub-modes:

1. First sub-mode: Before every turn on of the power device, the voltage on the capacitor C goes through 0V from the positive to negative direction, while the voltage over C_F is negative. In the second case it goes from the negative to positive direction, while the voltage over C_F is positive. The current through the resonant inductance is positive, while in the second case it is negative. After the switching on of the power device, during the time interval t_{ON} the current through the resonant inductance and power device changes its direction. The time t_{ON} is the bidirectional switch turn-on time.
2. Second sub-mode: Before every turn on of the power device the voltage on the capacitor C tries to go through 0V from the positive to negative direction, while the voltage over C_F is positive. In the second case it goes from the negative to positive direction, while the voltage over C_F is negative. The current through the resonant inductance is positive, while in the second case it is negative. After switching on the power device, during the time interval t_{ON} the current through the resonant inductance and power device does not changes its direction.

A. First Sub-Mode of Operation

The work of the converter is described with the timing diagrams shown in Fig. 3. The time T_S is a switching period.

The control signal from the generator u_{CG}, the control signal for the bidirectional power device u_{CD}, the resonant inductor current i_L, the bidirectional power device current i_{SW}, the bidirectional power device voltage u_{SW}, and the resonant capacitor voltage u_C are shown.

At the time t_1 the control signal u_{CG} reaches the level for switching on. The signal u_{CD} for switching on the power device is submitted only at t_2, when the voltage u_{SW} of the power device is equal to 0V. The input voltage is positive and after switching on the power device the voltage u_C on the resonant capacitor reaches the value u_S. Before switching on the power device the current through the inductor is negative and during the time t_{ON} it changes its direction.

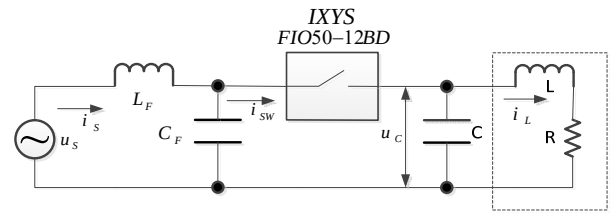

Fig. 2. Practical design of the converter.

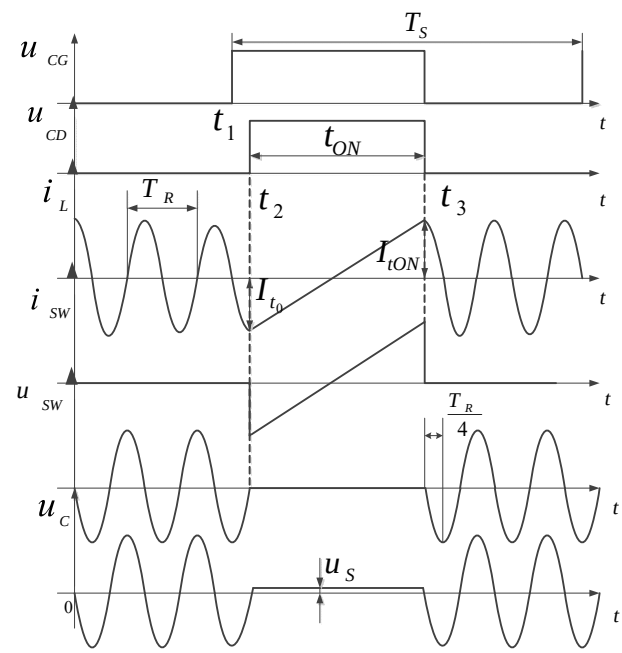

Fig. 3. Waveforms for the first sub mode. From top to bottom: control signal from the generator u_{CG}, control signal for the bidirectional power device u_{CD}, resonant inductor current i_L, bidirectional power device current i_{SW}, bidirectional power device voltage u_{SW}, and resonant capacitor voltage u_C.

The analysis in one switching period T_S is divided into two intervals: the first with a duration of t_{ON}, and the second is $(T_S - t_{ON})$. The aim is to obtain expressions for the basic values during both intervals: the current through the inductance, the voltage of the capacitor and the current through the bidirectional switch.

For the first interval with a duration of t_{ON} the current through the load inductance changes from I_{t_0} to $I_{t_{ON}}$. The value of the voltage of the capacitor is constant, and equal to the momentary value of the input voltage u_S (due to the high switching frequency of the power device):

$$u_C = u_S \tag{1}$$

The differential equation has the form of:

$$u_S = L.\frac{di_L}{dt} + R.i_L \tag{2}$$

From the initial condition:

$$i_L(t = 0) = I_{t_0} \tag{3}$$

it is determined that the integration time constant and this give:

$$i_L(t) = \frac{u_S}{R} + \left(I_{t_0} - \frac{u_S}{R}\right).e^{-\frac{t}{\tau}}, \tag{4}$$

where $\tau = \frac{L}{R}$ is the time constant.

The current value at the end of the interval is:

$$i_L(t_{ON}) = I_{tON} = \frac{u_S}{R} + \left(I_{t_0} - \frac{u_S}{R}\right).e^{-\frac{t_{ON}}{\tau}} \quad (5)$$

Assuming a sufficiently high frequency of the free current oscillations (a very small resonant period T_R) and a low attenuation $\delta = \frac{R}{2.L}$ in the resonance circuit, the currents at the beginning and end of the interval are approximately equal in absolute value but they are opposite:

$$I_{t_0} \approx -I_{tON} \quad (6)$$

As noted, equation (6) is valid under the assumption that the maximum values of the two adjacent half-waves with the same polarity as the volatility of the current through the resonant inductance are approximately equal.

Then from equation (5) it follows that:

$$I_{tON} = \frac{u_S}{R}.\frac{1-e^{-\frac{t_{ON}}{\tau}}}{1+e^{-\frac{t_{ON}}{\tau}}} \approx \frac{u_S}{R}.\frac{\frac{t_{ON}}{\tau}}{2-\frac{t_{ON}}{\tau}} \quad (7)$$

In this interval the current through the inductor is equal to the current through the bidirectional device. Therefore, equation (7) is valid also for the current of the device. In addition, using equation (7) it can determined the maximum of the current through the inductor and power device, considering the maximum voltage of the power source u_{Sm} and maximum time of switching on t_{ONm}:

$$I_{SWm} = I_{Lm} = I_{tONm} \approx \frac{U_{Sm}}{R}.\frac{\frac{t_{ONm}}{\tau}}{2-\frac{t_{ONm}}{\tau}} \quad (8)$$

For the second interval with a duration of $(T_S - t_{ON})$ the current changes from I_{tON} to I_{t_0} according to the oscillations rules. The last value is used as the initial value in the next switching period.

In this interval, the capacitor C is assumed to be ideal, its series resistance (ESR) is not considered and it is presumed that the resonance circuit maintains the same resistance R, which is connected in series with the inductor L. The differential equation has the form:

$$L.\frac{di_L}{dt} + R.i_L + \frac{1}{C}.\int i_L.dt = 0 \quad (9)$$

The solution is:

$$i_L(t) = e^{-\delta.t}.\left(C1.cos\sqrt{\omega_R^2 - \delta^2}.t + C2.sin\sqrt{\omega_R^2 - \delta^2}.t\right) \quad (10),$$

where $\delta = \frac{R}{2.L}; \omega_R = \frac{1}{\sqrt{L.C}}$

Accepting that $\omega_0 = \sqrt{\omega_R^2 - \delta^2}$ (11)

$$i_L(t) = e^{-\delta.t}(C1.cos\omega_0.t + C2.sin\omega_0.t) \quad (12)$$

The integration constants $C1$ and $C2$ are determined by the following conditions:

$$i_L(t=0) = I_{tON} \rightarrow C1 = I_{tON} \quad (13)$$

$$i_L\left(t \approx \frac{T_R}{4}\right) = 0 \rightarrow C2 = -I_{tON}.cotg\omega_0.\frac{T_R}{4} \quad (14)$$

Through integration the capacitor voltage variation is obtained:

$$u_C(t) = \frac{1}{C}.\int i_L(t).dt \quad (15)$$

i.e.:

$$u_C(t) = \frac{e^{-\delta.t}}{C.\omega_R^2}[(C1.\omega_0 - C2.\delta).sin\omega_0.t - (C2.\omega_0 + C1.\delta).cos\omega_0.t] \quad (16)$$

Its maximum value for this switching cycle is:

$$u_C\left(t \approx \frac{T_R}{4}\right) = u_{Cm} \rightarrow u_{Cm} = \frac{e^{-\delta\frac{T_R}{4}}}{C.\omega_R^2}.\left[(C1.\omega_0 - C2.\delta).sin\omega_0.\frac{T_R}{4} - (C2.\omega_0 + C1.\delta).cos\omega_0.\frac{T_R}{4}\right] \quad (17)$$

The maximum value of the voltage over the capacitor will correspond to the maximum value of the constants C1 and C2, and therefore to the maximum value of the currents through the inductance and the power device, defined by (8). Considering (8) (13) (14) and (17) it can be written that:

$$U_{Cm} \approx \frac{e^{-\delta\frac{T_R}{4}}}{C.\omega_R^2}.\left[(C1m.\omega_0 - C2m.\delta).sin\omega_0.\frac{T_R}{4} - (C2m.\omega_0 + C1m.\delta).cos\omega_0.\frac{T_R}{4}\right] \quad (18)$$

B. Second Sub-Mode of Operation

The operation of the converter in this mode is explained by the timing diagrams in Figure 4. The control signal from the generator u_{CG}, the control signal for the bidirectional power device u_{CD}, the resonant inductor current i_L, the resonant inductor current i_{SW} and the resonant capacitor voltage u_C are shown.

At the time t_1 the control signal u_{CG} reaches the level for switching on. The signal for switching the power device u_{CD} is submitted only at the moment t_2, when the voltage on the power device u_{SW} is equal to 0V. The input voltage is positive and after switching on the power device the voltage of the resonant capacitor u_C reaches the value u_S. Before switching on the power device current through the inductor is positive, and over time t_{ON} does not change its direction.

For the first interval with a duration of t_{ON} the current through the load inductance changes from I_{t_0} to $I_{t_{ON}}$. The value of the capacitor voltage is constant, and equal to the momentary value of the input voltage u_S (due to the high switching frequency of the power device):

$$u_C = u_S \quad (19)$$

The differential equation has the form of:

$$u_S = L.\frac{di_L}{dt} + R.i_L \quad (20)$$

From the initial condition:

$$i_L(t=0) = I_{t_0} \quad (21)$$

it is determined that the integration time constant and this give:

$$i_L(t) = \frac{u_S}{R} + \left(I_{t_0} - \frac{u_S}{R}\right).e^{-\frac{t}{\tau}}, \quad (22)$$

where $\tau = \frac{L}{R}$

The current value at the end of the interval is:

$$i_L(t_{ON}) = I_{tON} = \frac{u_S}{R} + \left(I_{t_0} - \frac{u_S}{R}\right).e^{-\frac{t_{ON}}{\tau}} \quad (23)$$

Supposing a sufficiently high frequency of free oscillations of the current (a very small resonant period T_R) and a low attenuation $\delta = \frac{R}{2.L}$ in the resonance circuit, it can be assumed that the currents at the beginning and end of the interval are

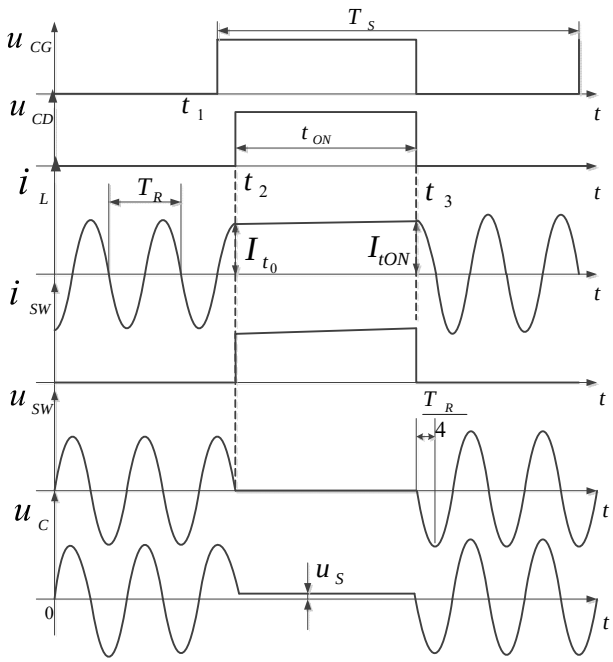

Fig. 4. Waveforms for the second sub mode. From top to bottom: control signal from the generator u_{CG}, control signal for the bidirectional power device u_{CD}, resonant inductor current i_L, bidirectional power device current i_{SW}, bidirectional power device voltage u_{SW}, and resonant capacitor voltage u_C.

approximately equal and have the same direction:

$$I_{t_0} \approx I_{tON} \tag{24}$$

As noticed equation (24) is valid under the assumption that the maximum values of the two adjacent half-waves with the same polarity as the volatility of the current through the resonant inductance are approximately equal.

Then from equation (23) it follows that:

$$I_{tON} = \frac{u_S}{R} \cdot \frac{1-e^{-\frac{t_{ON}}{\tau}}}{1-e^{-\frac{t_{ON}}{\tau}}} \approx \frac{u_S}{R} \tag{25}$$

In this interval the current through the inductor is equal to the current through the bidirectional device, and equation (25) is valid for the current of the device. Therefore, it is possible to determine the maximum value of the current through the inductance and the power device, considering the maximum voltage of the power source u_{Sm}:

$$I_{SWm} = I_{Lm} = I_{tONm} \approx \frac{U_{Sm}}{R} \tag{26}$$

For the second interval with a duration of $(T_S - t_{ON})$, equations (9) to (18) remain valid. This takes into account (25) in determining the constants C1 and C2 (13) and (14). In this interval the capacitor C is assumed to be ideal, its equivalent in series resistance (ESR) is not considered and it is presumed that the resonance circuit maintains the same resistance R, which is connected in series with the inductor L.

Comparing (8) and (26) it can be seen that in the second sub-mode the currents through the inductance and the power device are higher. The same is valid for the voltage over the resonance capacitor, which is described in (18).

As a conclusion of the mathematical description, the conditions can be summarized. The logarithmic decrement θ_{i_L} of the current oscillations i_L through the resonance inductance is equal to the logarithm of the ratio of the two adjacent maximum values of the same polarities.

$$\theta_{i_L} \approx ln \frac{I_{Lm}.e^{-\delta.t}}{I_{Lm}.e^{-\delta(t+T_R)}} = \delta.T_R \tag{27}$$

In the above equation the influence of δ on ω_0 is neglected. Therefore, the period of the oscillations in Figure 3 and Figure 4 are marked with T_R.

In order to have the maximum values of two neighboring half-waves with the same polarity as the current through the resonance inductance, the logarithmic decrement has to go to zero:

$$\theta_{i_L} \approx \delta.T_R \to 0 \tag{28}$$

Taking into account that $\delta = \frac{R}{2.L}; \omega_R = \frac{1}{\sqrt{L.C}}$, it follows:

$$\theta_{i_L} \approx \delta.T_R = \frac{R}{2.L}.2.\pi.\sqrt{L.C} = \pi.R.\sqrt{\frac{C}{L}} \to 0 \tag{29}$$

From (29) it follows that the value of the resonance capacitor and the equivalent resistance in the series resonance circuit must be as small as possible.

Therefore, from Fig. 3 and Fig. 4 it is clear that the effective duty ratio of the switch is reduced to $\frac{t_{ON}}{T_S}$ from the actual control signal duty ratio of $\frac{t_2-t_1+t_{ON}}{T_S}$. The maximum reduction of the duty ratio is $\frac{T_R}{2}$. In this are the only discrete values of the duty ratio. This is a drawback of the proposed technique. On the other hand, from Fig, 3, Figure 4 and the description of the switching at zero voltage, it is clear that the higher the ratio $\frac{T_S}{T_R}$ becomes, the larger the number of possible levels of power control. Then a period T_S will contain more half periods $\frac{T_R}{2}$ with more possibilities of switching on zero voltage.

III. A STUDY BY COMPUTER SIMULATION

The software product PSIM was used in this study. The simulation scheme is shown in Fig. 5. The voltage of the power device is monitored by isolating the amplifier and it is compared to 0V via the comparator. At each 0V crossing, the multivibrator controlled by the comparator generates short pulses (with a logical level 1). By connecting an RS-flip-flop and logic elements, the switching is guarantee despite the early control pulse generation from the generator. The flip-flop and logic elements provide the off of the power device immediately upon termination of the control pulse (logical level 0).

The simulation was performed under the following parameters: maximum voltage of the power source 325V, frequency 50 Hz, value of the resonant inductance 100 μH, equivalent series resistance 0.1Ω, output resistance 0.6 Ω, value of the capacitor of the resonance circuit 10 nF, equivalent series resistance 0.9 Ω, value of the switching frequency 20 kHz, value of the filter capacitor 20μF, and filter inductance

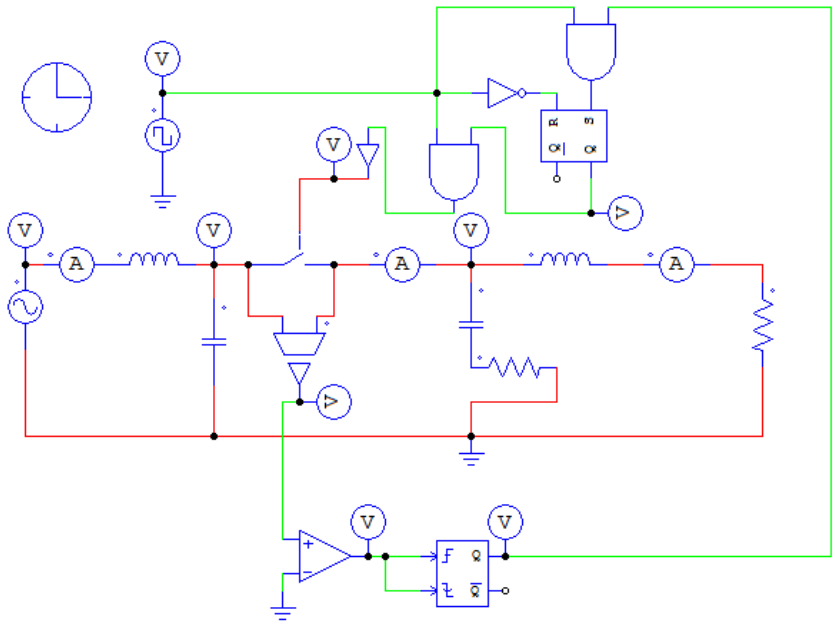

Fig. 5. Circuit for the computer simulation.

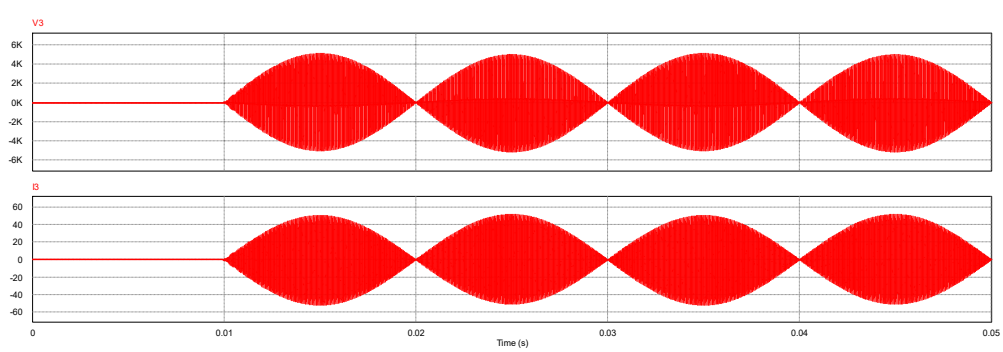

(a)

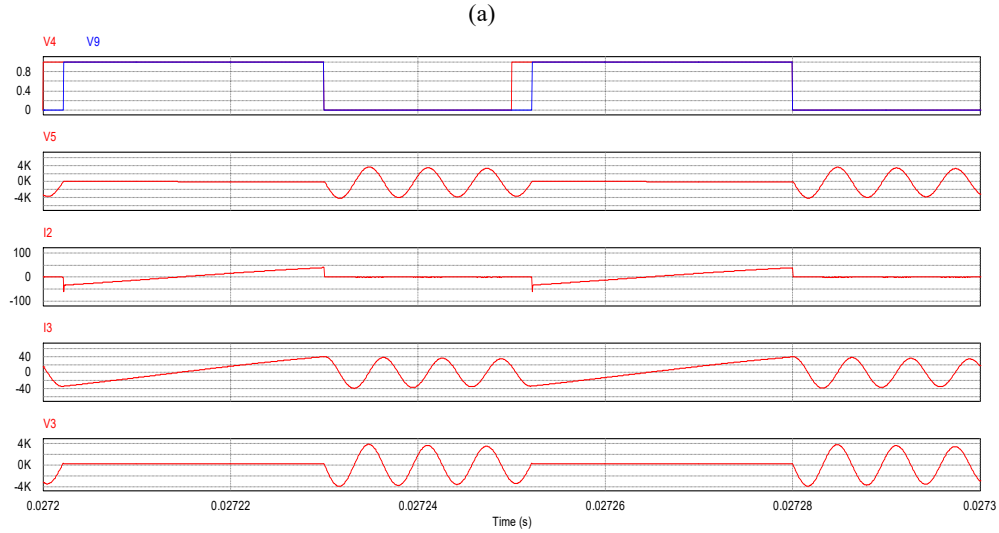

(b)

Fig. 6. Results at $D = 0.6$ - positive half period of the voltage on C_F (from 0.0272 s to 0.0273 s): a) $V3$ - resonant capacitor voltage, $I3$ - resonant inductor current; b) control signal from the generator $V4$, control signal for the bidirectional power device $V9$, bidirectional power device voltage $V5$, bidirectional power device current $I2$, resonant inductor current $I3$, resonant capacitor voltage $V3$.

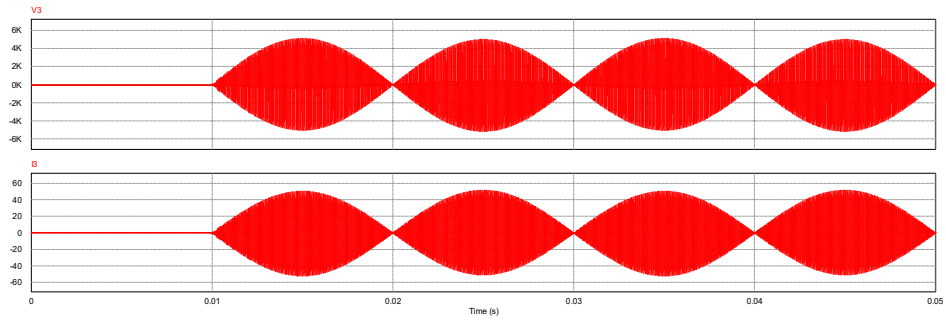

(a)

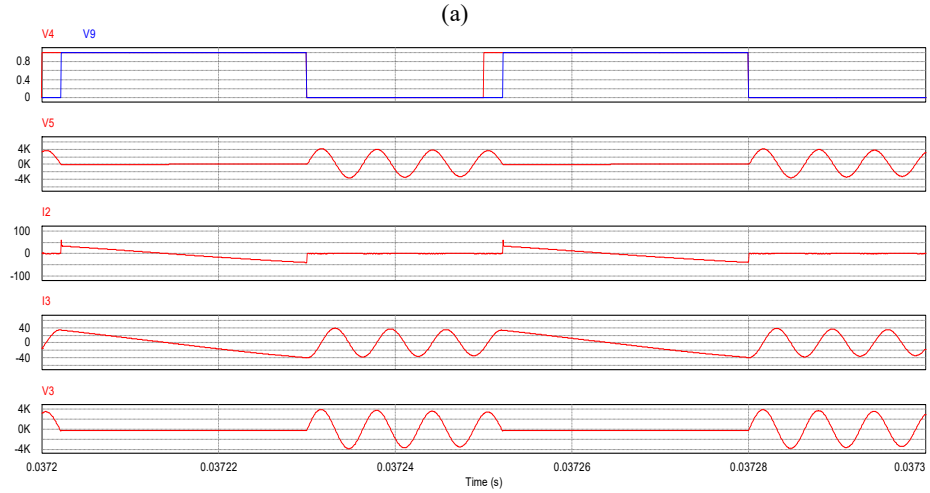

(b)

Fig. 7. Results at $D = 0.6$ - negative half period of the voltage on C_F (from 0.0372 s to 0.0373 s): a) $V3$ - resonant capacitor voltage, $I3$ - resonant inductor current; b) control signal from the generator $V4$, control signal for the bidirectional power device $V9$, bidirectional power device voltage $V5$, bidirectional power device current $I2$, resonant inductor current $I3$, resonant capacitor voltage $V3$.

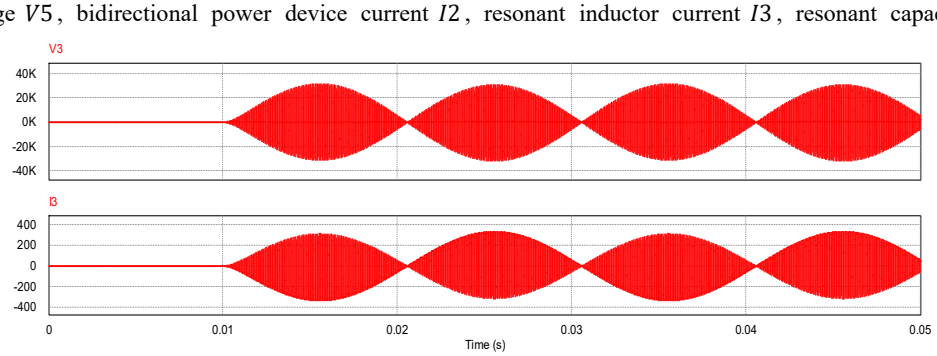

(a)

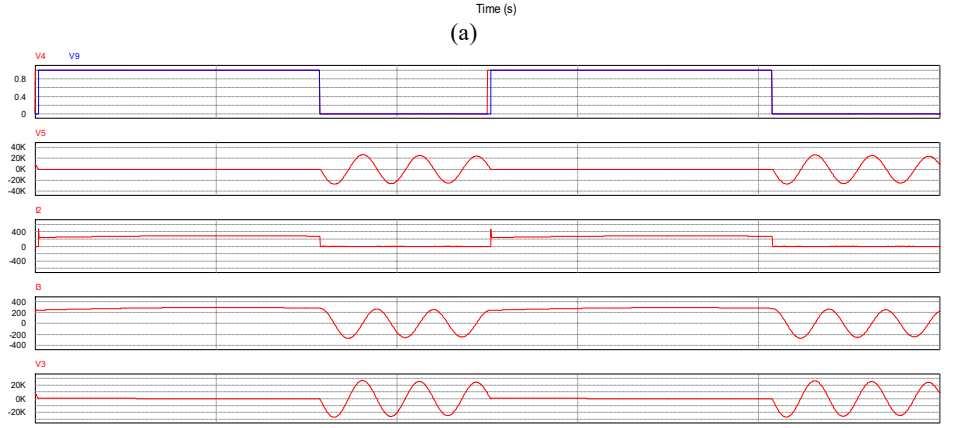

(b)

Fig. 8. Results at $D = 0.63$ - positive half period of the voltage on C_F (from 0.0272 s to 0.0273 s): a) $V3$ - resonant capacitor voltage, $I3$ - resonant inductor current; b) control signal from the generator $V4$, control signal for the bidirectional power device $V9$, bidirectional power device voltage $V5$, bidirectional power device current $I2$, resonant inductor current $I3$, resonant capacitor voltage $V3$.

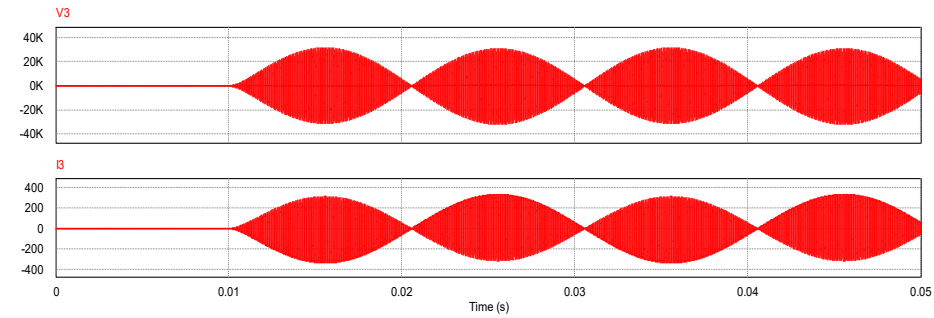

(a)

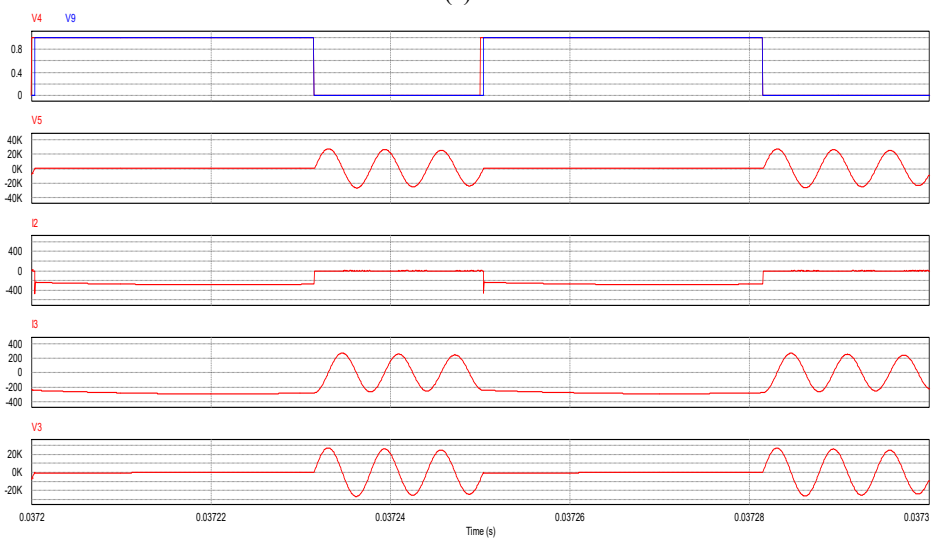

(b)

Fig. 9. Results at $D = 0.63$ - negative half period of the voltage on C_F (from 0.0372 s to 0.0373 s): a) $V3$ - resonant capacitor voltage, $I3$ - resonant inductor current; b) control signal from the generator $V4$, control signal for the bidirectional power device $V9$, bidirectional power device voltage $V5$, bidirectional power device current $I2$, resonant inductor current $I3$, resonant capacitor voltage $V3$.

value 680 μH. The duty cycle of control pulses D at a constant frequency is modified, i.e. the time t_{ON} has been changed.

A. First Sub-Mode of Operation

Fig. 6 and Fig. 7 show simulation results with a duty cycle of $D = \frac{t_{ON}}{T_S} = 0.6$ in the positive and negative half period of the voltage over C_F, respectively.

B. Second Sub-Mode of Operation

Fig. 8 and Fig. 9 show simulation results with a duty cycle of $D = \frac{t_{ON}}{T_S} = 0.63$ in the positive and negative half period of the voltage over C_F, respectively.

Comparing the results of the two sub-modes it is clear that the second sub-mode has significantly greater values for the currents through the circuit and power device, as well as the voltages over the device and resonance capacitor.

IV. Experimental Study

An experimental study of the converter from Fig. 2 has been carried out. In the initial experiments, the components of the schema were chosen to be the same as those in the computer simulation. The value of the filter capacitor was 20μF, and the value of the filter inductance was 680 μH. In reality, the actual values differ from the design. The measurement done with an RLC meter shows that the used resonant inductor L has a value of 93μH in the range of 20 kHz to 160 kHz. The resistance value of its equivalent series circuit at 160 kHz is 0.6Ω. The measurement with an RLC meter also indicates that the value of the capacitor C in the resonance circuit is 11nF, and its equivalent resistance (ESR) is 0.89Ω. The switching frequency of the converter managed from the generator in the control system is 20 kHz. Bidirectional power devices FIO50-12BD from IXYS Corporation were used. The control system was designed with CMOS ICs following the computer simulation. The power supply voltage frequency was 50 Hz. The currents on all of the waveforms (the second oscilloscope channel CH2) are in scale 100mV / A.

The first sub-mode waveform diagrams are shown in Fig. 10, Fig. 11, Fig. 12 and Fig. 13.

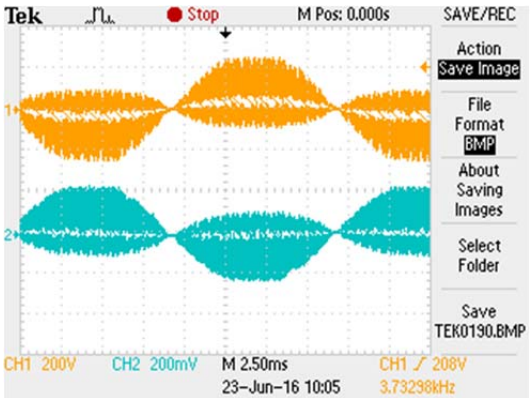

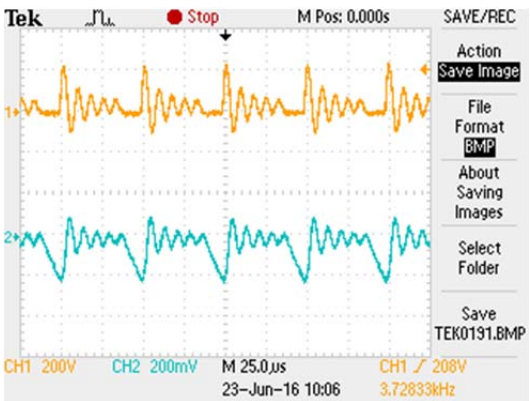

Fig. 10. First sub-mode by $L = 93\mu H$: CH1 – bidirectional power device voltage, CH2 – resonant inductor current.

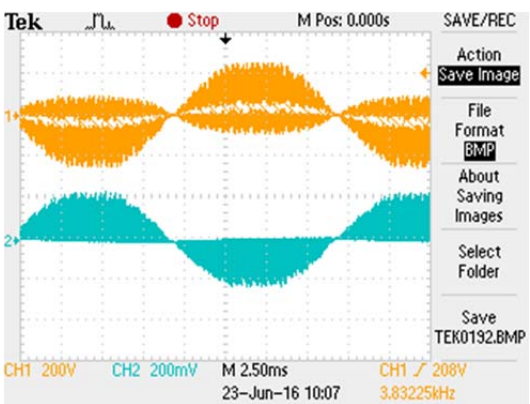

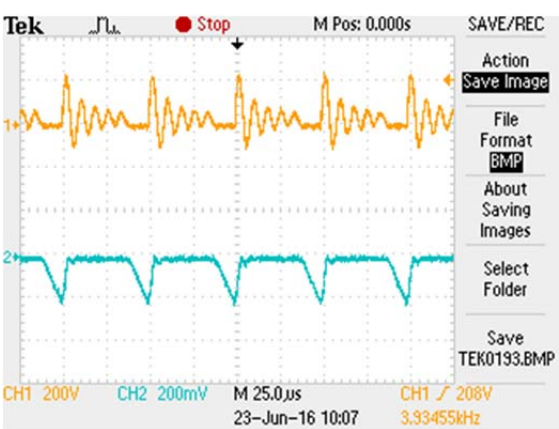

Fig. 11. First sub-mode by $L = 93\mu H$: CH1 – bidirectional power device voltage, CH2 – bidirectional power device current.

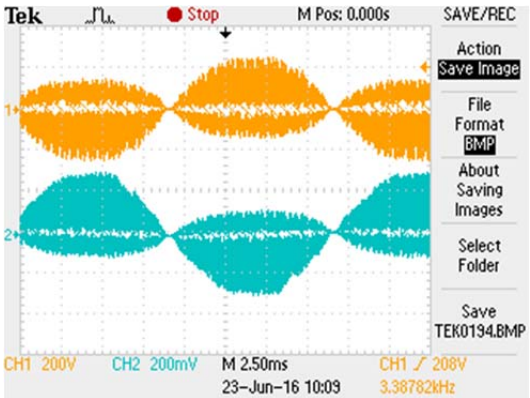

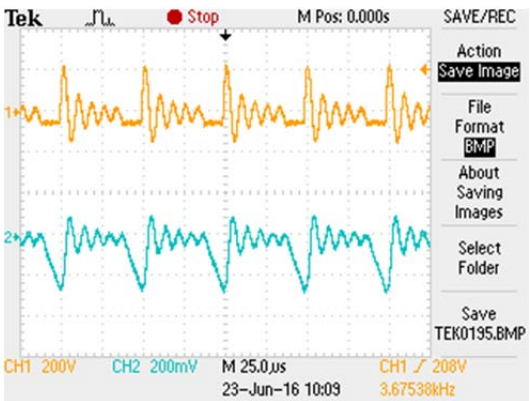

Fig. 12. First sub-mode by $L = 93\mu H$: CH1 – resonant capacitor voltage, CH2 – resonant inductor current.

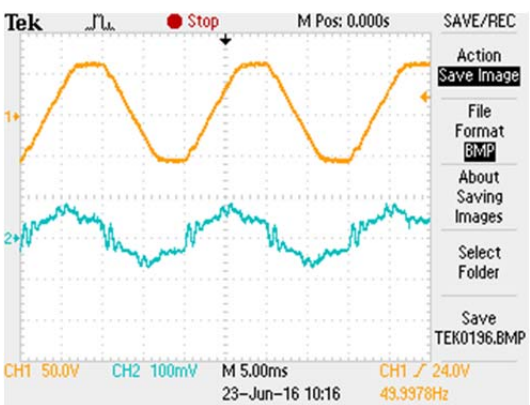

Fig. 13. First sub-mode by $L = 93\mu H$: CH1 – AC power source voltage, CH2 – AC power source current.

The second sub-mode waveform diagrams are shown in Fig. 14, Fig. 15, Fig. 16, and Fig. 17.

The increased resistance value in the resonance circuit used in the experiments when compared to the computer simulation provokes a higher attenuation in the circuit at high frequencies. This increased resistance value is due to the higher equivalent resistance of the resonant inductance and the equivalent resistance of the resonance capacitor. During the second interval with a duration of $(T_S - t_{ON})$ both of the resistances appear in series and increase the damping coefficient. Therefore, it is difficult to distinguish the two sub-modes.

Further experiments were carried out with a resonant

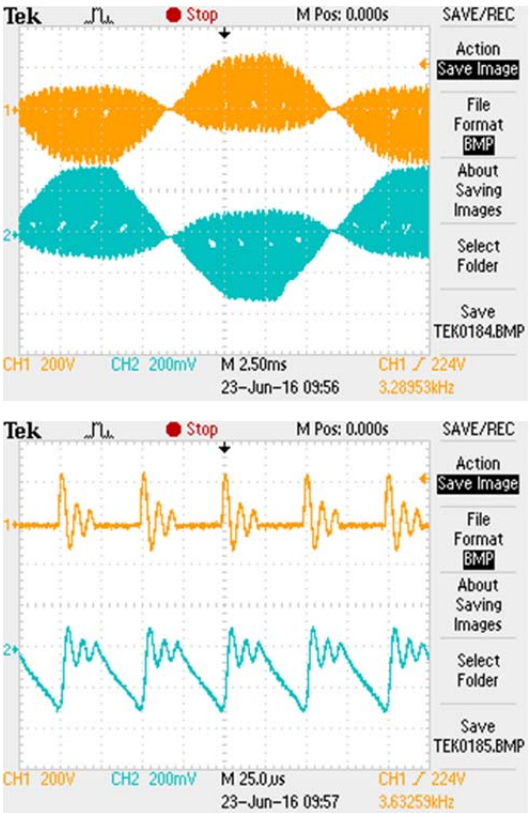

Fig. 14. Second sub-mode by $L = 93\mu H$: CH1 – bidirectional power device voltage, CH2 – resonant inductor current.

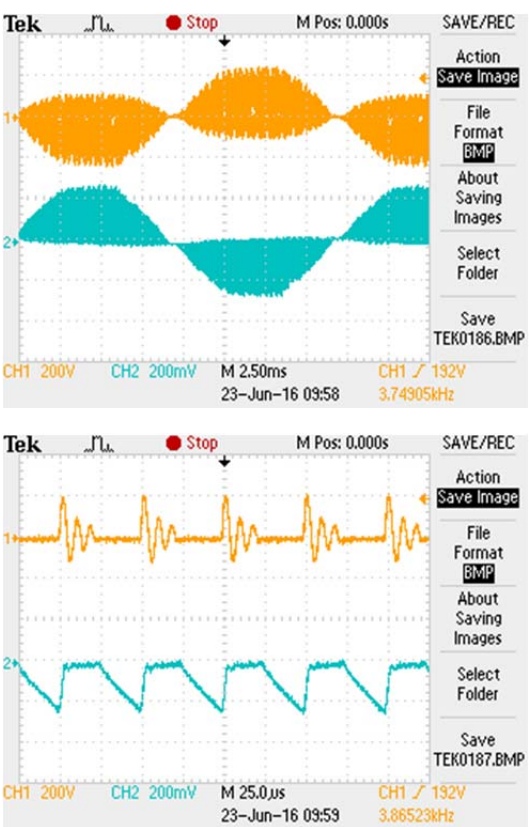

Fig. 15. Second sub-mode by $L = 93\mu H$: CH1 – bidirectional power device voltage, CH2 – bidirectional power device current.

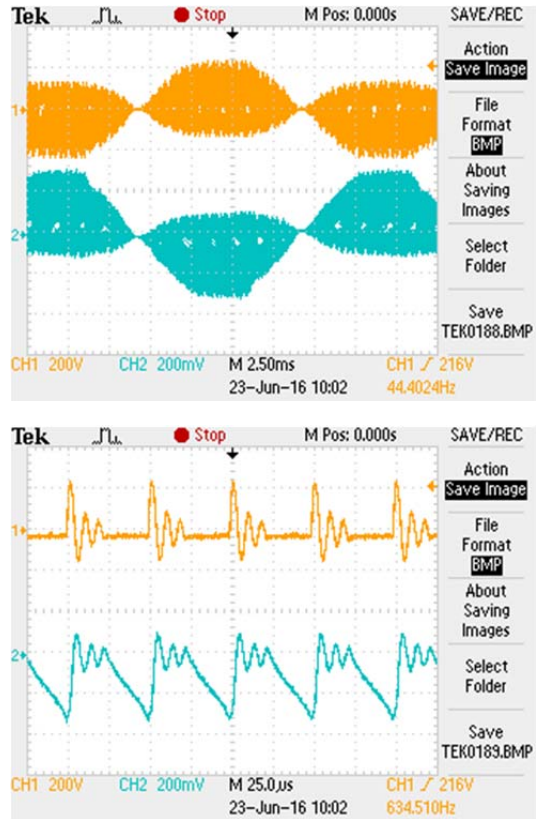

Fig. 16. Second sub-mode by $L = 93\mu H$: CH1 – resonant capacitor voltage, CH2 – resonant inductor current.

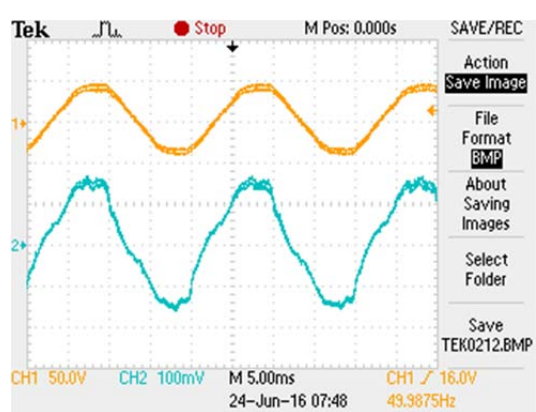

Fig. 17. Second sub-mode by $L = 93\mu H$: CH1 – AC power source voltage, CH2 – AC power source current.

inductance value of 360µH and an equivalent series resistance of 1.5Ω. As a result, both sub-modes can be more easily distinguished.

The first sub-mode waveform diagrams are shown in Fig. 18, Fig. 19, Fig. 20, and Fig. 21.

A supply source current with a nearly sinusoidal shape is achieved in all of the experimental cases. The phase advancement with respect to the voltage is due to the capacitor C_F . Through the optimization of the filter for a specific practical case, a high power factor can be achieve in both sub-modes.

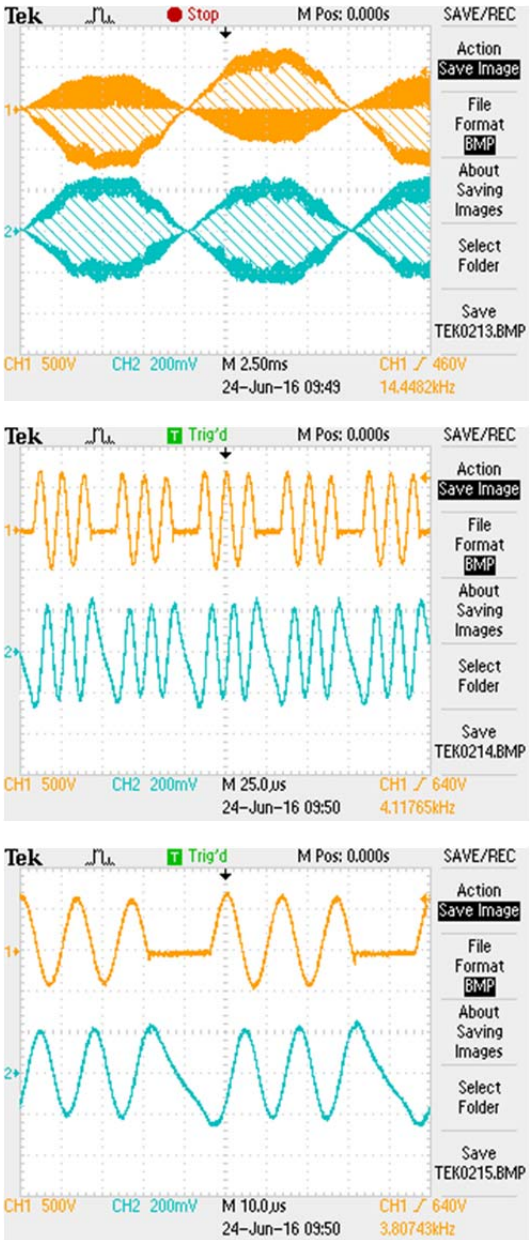

Fig. 18. First sub-mode by $L = 360\mu H$: CH1 – bidirectional power device voltage, CH2 – resonant inductor current.

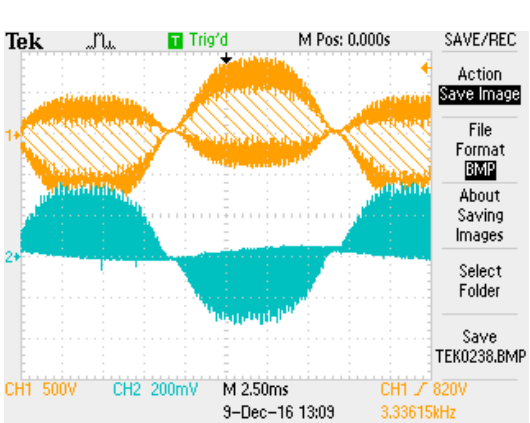

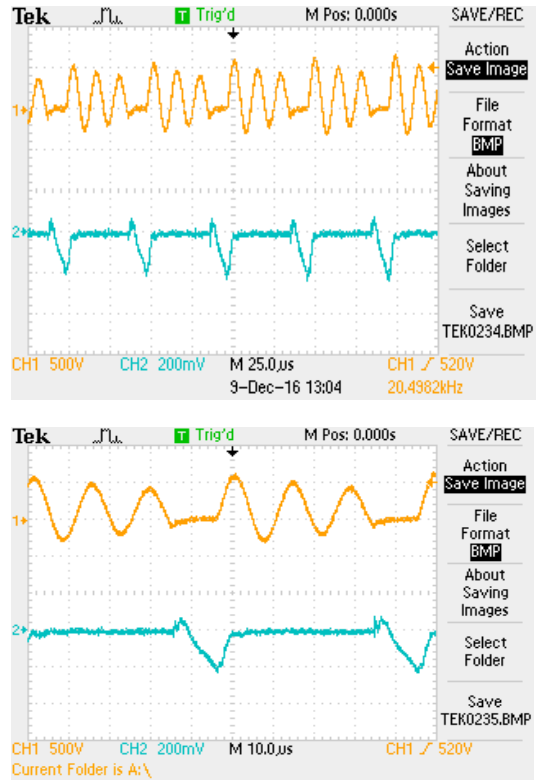

Fig. 19. First sub-mode by $L = 360\mu H$: CH1 – bidirectional power device voltage, CH2 – bidirectional power device current.

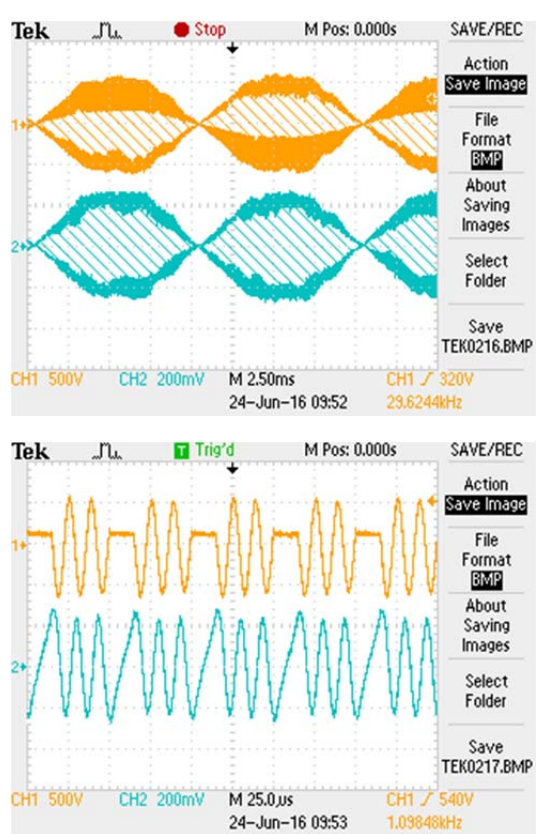

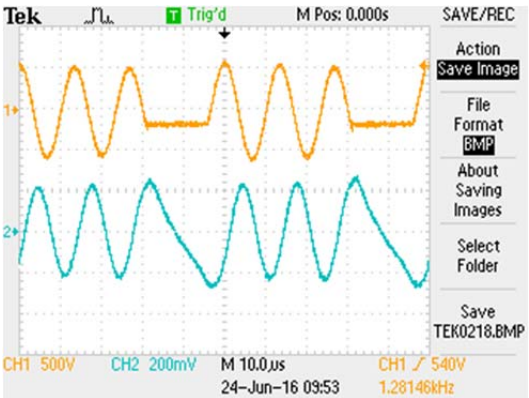

Fig. 20. First sub-mode by $L = 360\mu H$: CH1 – resonant capacitor voltage, CH2 – resonant inductor current.

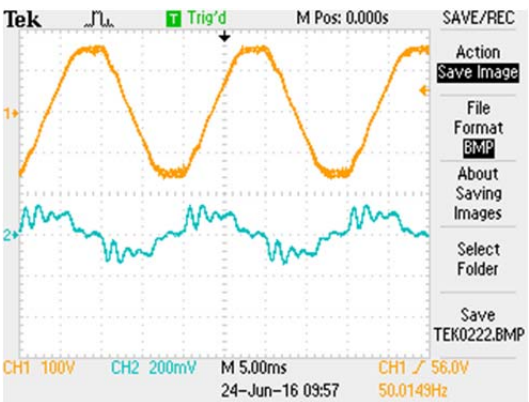

Fig. 21. First sub-mode by $L = 360\mu H$: CH1 – AC power source voltage, CH2 – AC power source current.

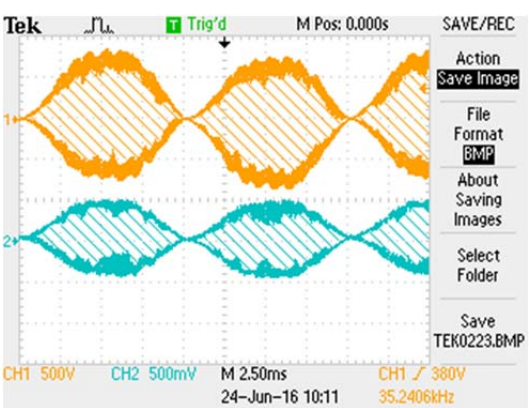

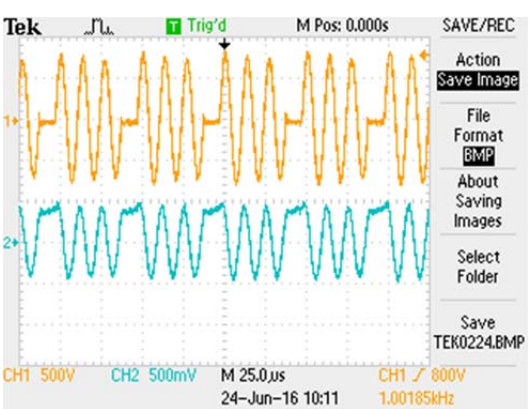

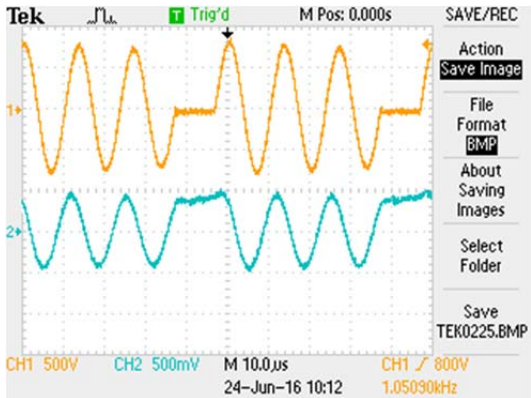

Fig. 22. Second sub-mode by $L = 360\mu H$: CH1 – bidirectional power device voltage, CH2 – resonant inductor current.

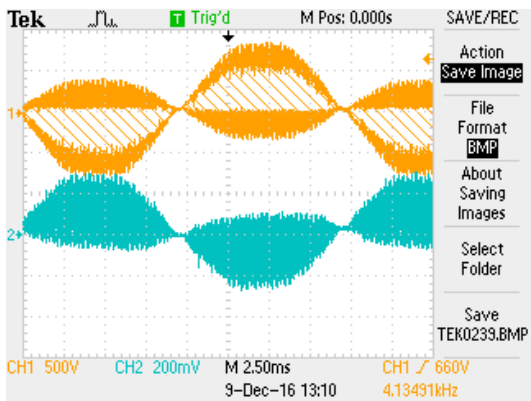

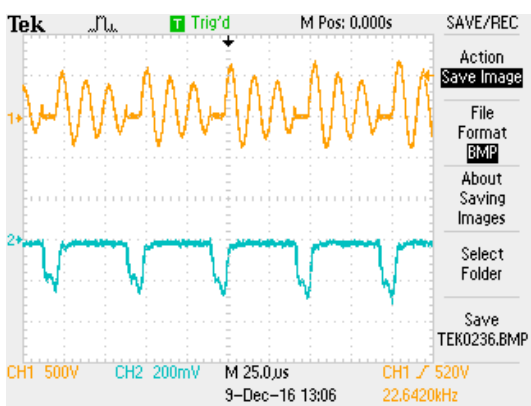

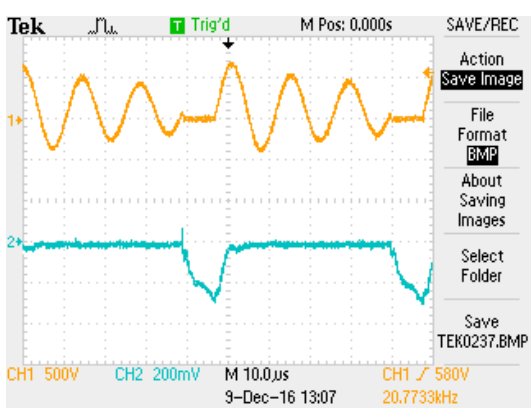

Fig. 23. Second sub-mode by $L = 360\mu H$: CH1 – bidirectional power device voltage, CH2 – bidirectional power device current.

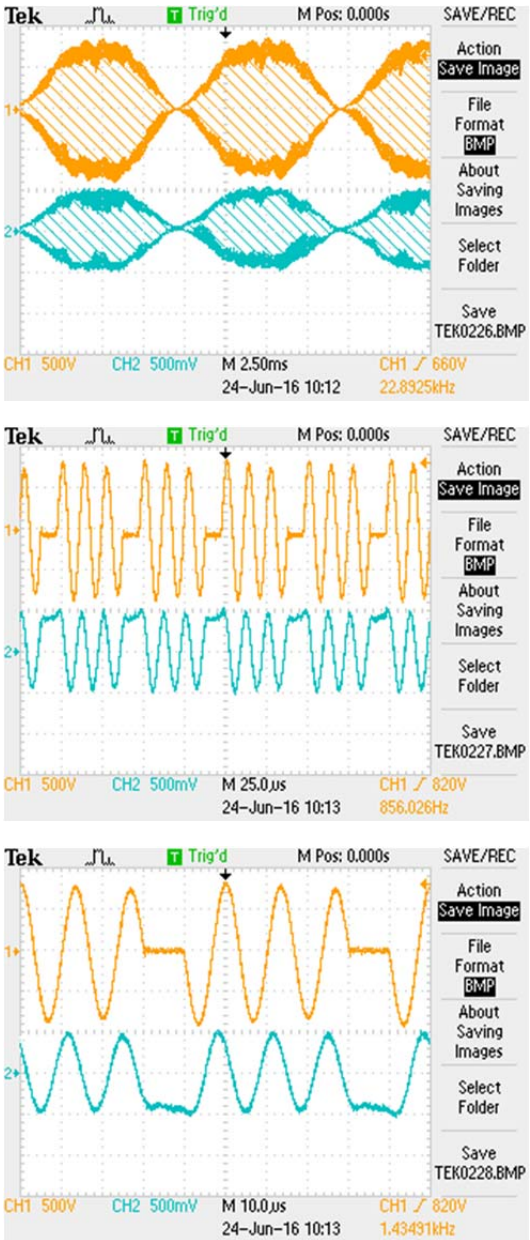

Fig. 24. Second sub-mode by $L = 360\mu H$: CH1 – resonant capacitor voltage, CH2 – resonant inductor current.

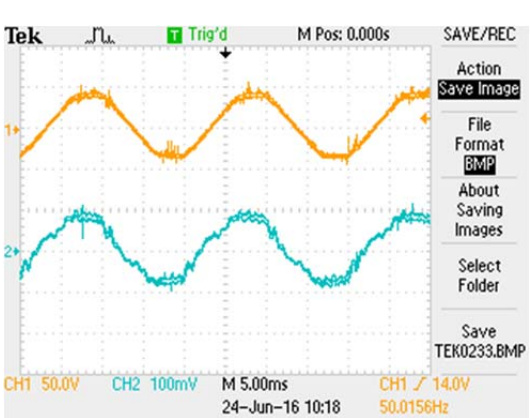

Fig. 25. Second sub-mode by $L = 360\mu H$: CH1 – AC power source voltage, CH2 – AC power source current.

The second sub-mode waveform diagrams are shown in Fig. 22, Fig. 23, Fig. 24 and Fig. 25.

V. CONCLUSION

A single-phase AC-AC converter using a bidirectional power device is described in this paper. The switching on of the device is done at zero voltage by simply monitoring its voltage, and the signal to control the device is applied to the gate after processing in the control system. The mode of the continuous current through the resonant inductance is studied, and two possible sub-modes were shown. A mathematical description, computer simulation and experimental studies are done for each of the sub-modes. The second sub-mode is characterized by a significant increase in the current through the load and the power device, and in the voltage over the resonance capacitor and the device. The advantages of this converter are its reduced losses due to the use of only one device and its implemented soft switching mechanism. There are possibilities for future investigations. For example, with a small change in the duty cycle of the control pulses to the bidirectional power device, is possible to change the converter from one sub-mode to the other, which causes step changes of the power to the load. This requires the development of a new regulation algorithm, where the power in the load is only adjusted in the first sub-mode by increasing the time for switching on the power device. Then increasing the power can only take place in the second sub-mode by increasing the time for switching on the power device. The possible converter applications are: induction heating and contactless inductive power transfer.

REFERENCES

[1] P. Chlebis, P. Simonik, and M. Kabasta, "The comparision of direct and indirect matrix converters," *Progress In Electromagnetics Research Symposium Proceedings*, pp. 310-313, 2010.

[2] Trentin, P. Zanchetta, J. Clare, and P. Wheeler, "Automated optimal design of input filters for direct AC/AC matrix converters," *IEEE Trans. Ind. Electron.*, Vol. 59, No. 7, pp. 2811-2822, Jul. 2012.

[3] M. Moghaddami, A. Anzalchi, and A. Sarwat, "Single-state three-phase AC-AC matrix converter for inductive power transfer systems," *IEEE Trans. Ind. Electron.*, Vol. 63, No. 10, pp. 6613-6622, May 2016.

[4] M. Antchev and G. Kunov, "Investigation on three- phase to single – Phase matrix converter," *Facta Universitatis, Ser. Electrical Engineering*, Vol. 22, No. 2, pp. 245-252, Aug. 2009.

[5] G. Kunov, M. Antchev, and E. Gadjeva, "Computer modeling of three-phase to single-phase matrix converter using MATLAB," *Electronics*, Vol. 14, No. 1, pp. 50-55, Jun. 2010.

[6] O. Lucia, C. Carrereto, J. M. Burdio, J. Acero, and F. Almazan, "Multiple-output resonant matrix converter for multiple induction heaters," *IEEE Trans. Ind. Appl.*, Vol.

48, No. 4, pp. 1387-1396, Jul./Aug. 2012.

[7] H. Sugimura, S. Mun, S. Kwon, T. Mishima, and M. Nakaoka, "High frequency resonant matrix converter using one-chip reverse blocking IGBT-based bidirectional switches for induction heating," *Power Electronics Specialist Conference Proceedings*, pp. 3960-3966, 2008.

[8] H. Sugimura, A. M. Eid, S. K. Kown, H. W. Lee, E. Hiraki, and M. Nakaoka, "High frequency cyclo-converter using one-chip reverse blocking IGBT based bidirectional power switches," *International Conference of Electrical Machines and Systems*, Vol. 2, pp. 1095-1100, 2005.

[9] H. Sugimura, S. P. Mun, S. K. Kwon, E. Hiraki, and M. Nkaoka, "Active voltage clamped edge-resonant soft switching PWM high frequency cyclo-converter using bidirectional switches," *IEEE Power Electronics Specialists Conference*, pp. 3917-3923, 2008.

[10] H. Sornago, O. Lucia, A. Mediano, and J. Burdio, "A Class-E direct AC-AC converter with multicicle modulation for induction heating systems," *IEEE Trans. Ind. Electron.*, Vol. 61, No. 5, pp. 2521-2531, May 2014.

[11] S. Aldhaher, P. Luk, and A. Bati, "Wireless power transfer using class E inverter with saturable DC-feed inductor," *IEEE Trans. Ind. Appl.*, Vol. 50, No. 4, pp. 2710-2718, Jul./Aug. 2014.

[12] Z. Kaczmarczyk, "A high-efficiency Class E inverter – computer model, laboratory measurement and SPICE simulation," *Bulletin of the Polish Academy of Sciences*, Vol. 55, No. 4, pp. 411-417, 2007.

[13] M. Bland, L. Emprinham , J. Clare, and P. Wheeler, "A new resonant soft switching topology for direct AC-AC COnverters," *Power Electronics Specialist Conference Proceedings*, pp. 72-77, 2002.

[14] H. Sornago, O. Lucia, A. Mediano, and J. Burdio, "Direct AC-AC resonant boost converter for efficient domestic induction heating application," *IEEE Trans. Power Electron.*, Vol. 29, No. 3, pp. 1128-1140, Mar. 2014.

[15] H. Sornago, O. Lucia, A. Mediano, and J. Burdio, "Efficient and cost – Effective ZCS direct AC-AC resonant converter for induction heating," *IEEE Trans. Ind. Electron.*, Vol. 61, No. 5, pp. 2546-2556, May 2014.

[16] R. Moghe, R. P. Kandula, A. Iyer, and D. Divan, "Losses in medium –Voltage megawatt-rated direct AC/AC power electronics converters," *IEEE Trans. Power Electron.*, Vol. 30, No. 7, pp. 3553-3562, Jul. 2015.

[17] H. L. Li, A. Hu, and G. Covic, "A direct AC-AC converter for inductive power- transfer systems," *IEEE Trans. Power Electron.*, Vol. 27, No. 2, pp. 661-669, Feb. 2012.

[18] H. L. Li, A. Hu, and G. Covic, "Current fluctuation analysis of a quantum ac-ac resonant converter for contactless power transfer," *Energy Conversion Congress and Symposium Proceedings*, pp. 1838-1843, 2010.

[19] X. Ju, L. Dong, X. Liao, and Y. Jin, "An AC-AC energy injection resonant converter for wireless power transfer applications," *Future Energy Electronics Conference (IFEEC)*, pp. 1-5, 2015.

[20] H. L. Li, P. A. Hu, and G. Covic, "A high frequency AC-AC converter for inductive power transfer (IPT) applications," *Wireless Power Transfer –principles and Engineering Explorations*, INTECH, Chapter 13, pp. 253-272, 2012.

[21] F. Kusumah, S. Vuorsalo, and J. Kyyra, "A direct three-phase to single-phase AC/AC converter for contactless electric vehicle charger," *European Power Electronics and Applications (EPE'15 ECCE-Europe)*, pp. 1-10, 2015.

[22] J. Itoh, T. Iida, and A. Odaka, "Realisation of high effiicency AC link converter system based on AC/AC direct conversion techniques with RB-IGBT," *32th Annual Conference on IEEE Industrial Electronics (IECON 2006)*, Paris, France, pp. 1703-1708, 2006.

[23] H. Benkaci, A. Cheriti, M. Benslima, and A.Sandali, "PDM control optimization applied to an AC/AC converter using an improved genetic algorithm," *Canadian Conference on Electrical and Computer Engineering*, pp.2232-2236, 2006.

[24] M. Antchev, "Analysis and Investigation of Direct AC-AC Quasi – Resonant Converter," *Americal Journal of Electrical Power and Energy Systems*, Vol. 4, No. 6-1, pp. 1-7, Dec. 2015.

Mihail Hristov Antchev was born in Sofia, Bulgaria, in 1955. He received his M.S., Ph.D. and D.Sc. degrees in Electronics from Technical University, Sofia, Bulgaria, in 1981, 1990 and 2011, respectively. From 1981 to 1985, he was a Researcher; from 1985 to 1993, he was an Assistant Professor; from 1993 to 2012, he was an Associate Professor; and he is presently a Professor in the Power Electronics Section of Technical University. His current research interests include the design and control of power electronic energy converters and systems, active power filters and UPS systems.